Dependence of the Confinement of Fast Ions Generated by ICRF Heating on the Field Configuration in Heliotron J

H. Okada 1), Y. Torii 2), S. Kobayashi 1), M. Kaneko 3), H. Kitagawa 3), T. Tomokiyo 3), T. Mutoh 4), T. Mizuuchi 1), K. Nagasaki 1), Y. Nakamura 3), S. Yamamoto 5), H. Arimoto 3), K. Hanatani 1), K. Kondo 3) and F. Sano 1)

1) Institute of Advanced Energy, Kyoto Univ., Gokasho, Uji, Kyoto 611-0011, Japan
2) High Temperature Plasma Center, Univ. Tokyo, 5-1-5 Kashiwa-no-ha, Kashiwa, Chiba 227-8568, Japan
3) Graduate School of Energy Science, Kyoto Univ., Gokasho, Uji, Kyoto 611-0011, Japan
4) National Institute of Fusion Science, 322-6 Oroshi-cho, Toki, Gifu 509-5292, Japan
5) Graduate School of Engineering, Osaka Univ., Suita, Osaka 565-0571, Japan

e-mail contact of main author: okada@iae.kyoto-u.ac.jp

Abstract A formation and confinement experiment for fast ions is performed using the ion cyclotron range of frequencies (ICRF) minority heating scheme with a proton minority and a deuteron majority in Heliotron J, a low-shear helical-axis heliotron. The effect of the magnetic configuration on the fast ion confinement is one of the most important issues in helical devices. In this paper, the effect of the bumpiness on the trapped fast ion confinement is clarified by using ICRF minority-heating. The role of one of the Fourier components, the bumpiness, is a key issue for the design principle of the magnetic filed of Heliotron J, where the particle confinement is controlled by the bumpiness. The proper bumpiness causes deeply trapped particles to be confined in the small grad-B region. Two loop antennas are installed on the low-field side of the corner section of Helitoron J. A high energy ions are produced up to 10 keV by injecting an ICRF pulse into an electron cyclotron heating (ECH) target plasma where ion temperature at the center $T_i(0)$ = 0.2 keV, electron temperature at the center $T_e(0)$ = 0.8 keV and line-averaged electron density $\bar{n}_e$ = 0.4x10^{19} m^{-3}. For the study of the configuration dependence of the fast particle confinement, three configurations are selected; the bumpy ripples (B_{04}/B_{00}, where B_{04} is the bumpy component and B_{00} is the averaged magnetic field strength) are 0.01, 0.06 and 0.15 at the normalized minor radius ρ = 0.67. The measured tail temperatures by using a charge-exchange neutral energy analyze are 1.04, 0.87 and 0.47 keV for the ripples of 0.15, 0.06 and 0.01, respectively. The heating efficiency of the bulk ion is also better in the high bumpy case.

1. Introduction

A formation and confinement experiment for fast ions is performed using the ICRF minority heating scheme with a proton minority and a deuteron majority in Heliotron J [1, 2], a low-shear helical-axis heliotron (major radius of the torus R_0 = 1.2 m, minor radius of the plasma a = 0.1-0.2 m, magnetic field on the axis $B_0 \leq$ 1.5 T, helical-coil pole number L = 1, pitch number M = 4). The design concept of Heliotron J is that high-energy particles should be confined sufficiently in the high beta region due to the good magnetohydrodynamic (MHD) characteristics. It is also an important subject for Heliotron J to seek the guiding principle for optimizing the confinement-field structure. Using controllable five sets of coil power supplies, Helitoron J realizes a wide range of configurations by changing the coil-current ratios. They are the helical coil connected serially to the main vertical coils, the outer vertical coils, the inner vertical coils, the toroidal A coils (stronger ones), and the toroidal B coils (weaker ones). The effect of the magnetic configuration on the fast ion confinement is one of the most important issues in helical devices. In this paper, the effect of the bumpiness on the trapped fast ion confinement is clarified by using ICRF minority-heating. The role of one of the Fourier components, the bumpiness, is a key issue for the design principle of the magnetic filed of Heliotron J, where the particle confinement is controlled by the bumpiness [3]. The bumpy component of the magnetic field is controlled by changing the current ratio of the toroidal A coils to the toroidal B coils. The proper bumpiness causes deeply trapped particles to be confined in the small grad-B region.

ICRF heating and NBI heating have been used to investigate the energetic ion confinement and the additional heating in Heliotron J. The fast ion confinement was studied using tangentially injected fast ions by using NBI, whose injection energy is 28 keV, in the previous work [4]. However, trapped particles were not sufficiently investigated in the NBI experiment. ICRF heating is supposed to be suitable for this type of experiment because of no additional particle source and the possibility of accelerating ions perpendicularly up to the high energy [5-8]. In this paper, fast ions generated using the ICRF heating in Heliotron J and resultant heating efficiency are described with special emphasis on the effect of the bumpy component of the magnetic field.

2. Experimental Setup

Figure 1 shows the experimental setup of the heating and diagnostic devices in

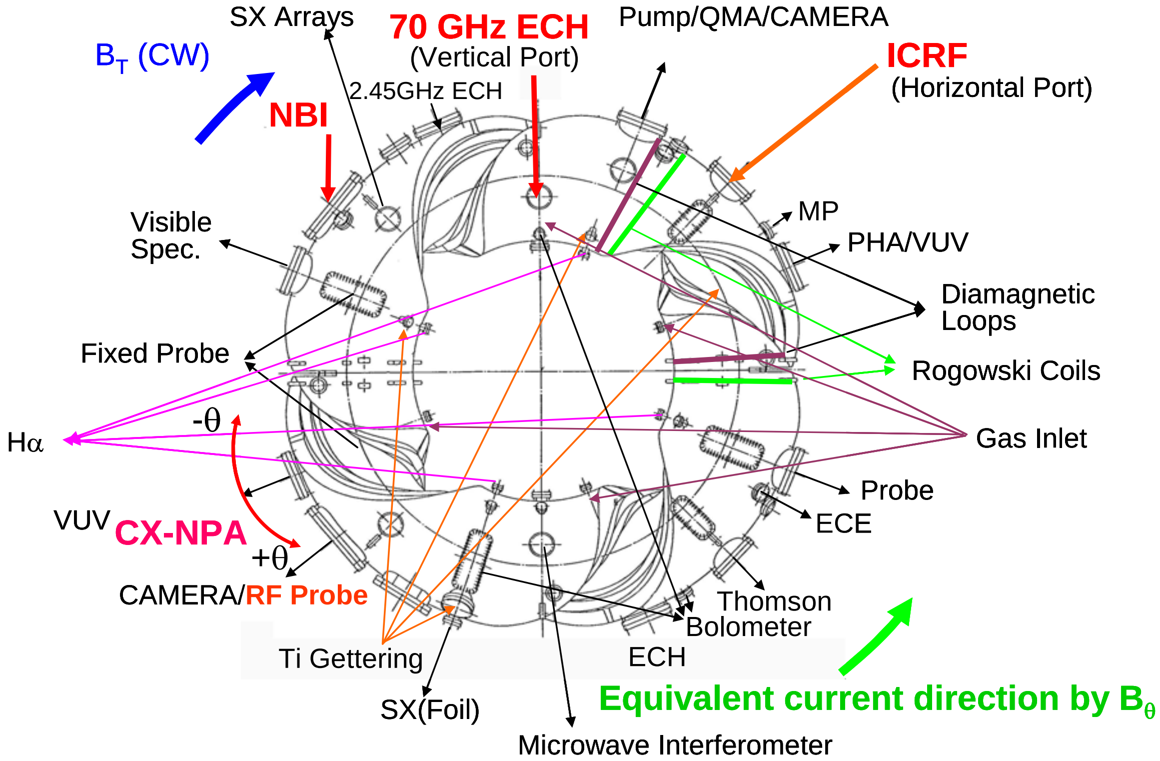

Fig. 1. Heating and diagnostic systems in Heliotron J. ICRF antennas are installed at the upper right corner.

Heliotron J. Plasmas are generated by using a 70-GHz ECH beam injected vertically from the upper port. Two ICRF loop antennas are installed in the poloidal cross section indicated in Fig. 2. This section corresponds to the corner section of a Heliotron J plasma, where the mod-B surface has a tokamak-like structure. The cyclotron-resonance layer is located near the axis with a frequency of 19 MHz in the STD configuration. The left-hand cutoff and the two-ion hybrid resonance layers are also presented in Fig. 2. The frequency is changed so that the resonance layer is shifted to the selected position. The frequency range applied in this experiment is from 19 to 23.2 MHz. The ICRF wave is radiated from the antenna on the low-field side to ECH target plasmas. The ECH power is in the range from 0.29 to 0.35 MW. Each antenna is fed by an independent transmitter. The phase between the two antenna currents can be controlled by a phase shifter. The poloidal wave number can be controlled by changing the phases of the ICRF currents. The antenna loop is made of stainless steel, and the carbon side guards are located on both sides of the antenna. The size of the antenna loop facing a plasma is 0.25 m (length) x 0.14 m (width). A single Faraday screen covers the antenna loop. The antenna resistance has been measured using a radio-frequency (rf) current pickup coil and an rf-voltage detector installed in a co-axial transmission line between the matching circuit and the antenna. The resistance due to the plasma loading is from 2.0 to 5.0 Ω in a line-averaged density range from 0.15 to 0.6 x 10^{19} m^{-3} when the lower antenna is used. These values agree with those calculated using numerical model under the minority-heating scheme [4].

A charge-exchange neutral-particle energy analyzer (CX-NPA) is equipped to analyze the energetic ions, which has the ability of scanning in the toroidal and poloidal directions in order to research ions in the wide range of the velocity distribution. The CX-NPA has 10 channels for hydrogen and 10 channels for deuterium. The type of the analyzer is *E//B*. The energy range is from 0.4 to 80 keV for hydrogen and from 0.2 to 40 keV for deuterium with the energy resolution in the range from 4 to 10%. It can be scanned in the toroidal direction from -10 to +18 deg and in poloidal direction from -3 to 10 deg in order to observe charge-exchange neutrals in the wide range of the velocity distribution. The origin is the normal direction to the torus for the toroidal angle and the horizontal direction for the poloidal angle. For the poloidal direction the CX-NPA is determined so that the line of

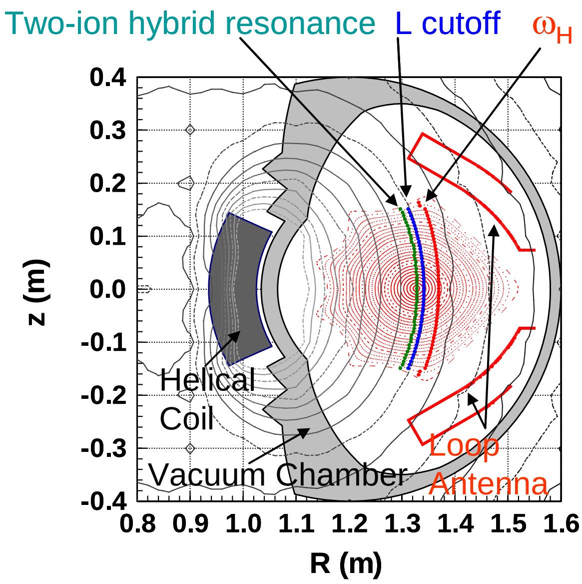

Fig. 2. A schematic view of two antenna loops, the plasma shape, the proton cyclotron-resonance layer (ω_H), the left-hand cutoff layer, the two-ion hybrid resonance layer, and the mod-B surface in the poloidal cross section at the corner section of Heliotrn J. The cutoff and resonance layers are calculated with the parameters: ICRF frequency = 19 MHz, density = 0.5 x 10^{19} m^{-3}, B_0 = 1.32 T, minority ratio = 0.1 and parallel wave number $k_{//}$ = 0.53 m^{-1}.

sight of the CX-NPA crosses the magnetic axis for every toroidal angle in this experiment. It is noted that the ions with various types of orbits are contained in the flux obtained by the CX-NPA along its line of sight, for example, passing particles, trapped particles and loss particles.

3. Dependence of the High-Energy Ion Formation and Confinement on the Bumpy Field Component

Fast-ion confinement is studied in relation to the magnetic configurations. It is predicted that one of the Fourier components of the magnetic field in the Boozer coordinates, the bumpy component (B_{04}), plays a key role on the collisionless-particle confinement in the Heliotron J configuration. Three configurations are selected; the bumpy ratio (B_{04}/B_{00}, where B_{00} is the averaged magnetic-field strength) are 0.01, 0.06 and 0.15 at the normalized minor radius $\rho = 0.67$. This experiment has been performed in the low-density deuteron plasmas (0.3 x 10^{19} to 0.5 x 10^{19} m^{-3}) with minority protons since the plasma should be collisonless. The ICRF frequency is adjusted so that the cyclotron-resonance layer may be positioned within $\rho = 0.2$. In the cases of B_{04}/B_{00} = 0.01, 0.06 and 0.15, the frequency is 19, 19 and 23.2 MHz, respectively. One loop antenna on the lower side is used in this experiment, and the injected power at the vacuum feed through is about 0.2 MW. The observed high-energy flux is largest in the case of the highest bumpy component and smallest for the lowest bumpy component as shown in Fig. 3a. The tail temperatures estimated from the slope of the energy spectra between 2.0 to 6.0 keV are 0.47, 0.87 and 1.04 keV for B_{04}/B_{00} = 0.01, 0.06 and 0.15, respectively. To understand this result, many aspects of the heating and diagnostics must be considered; they are the fast-ion formation, its confinement, the velocity-loss region along the CX-NPA's chord, and so on.

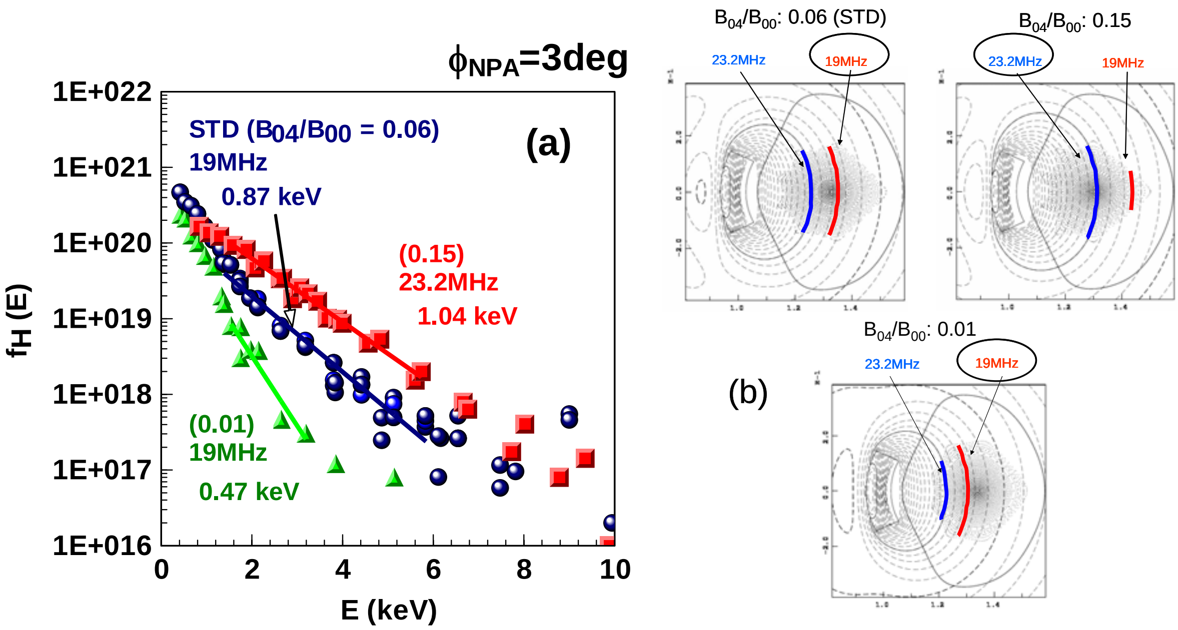

Fig. 3. (a) Energy spectra of the minority hydrogen for various bumpy components (B_{04}/B_{00}). (b) The field configuration, the mod-B surface, and the proton cyclotron-resonance layer in the poloidal cross section where the ICRF antennas are installed are presented for three bumpy components.

The injection power and the position of the cyclotron-resonance layer are almost same for the three cases in order to keep constant for the condition of the fast-ion formation as shown in Fig. 3b. Ions with various types of orbit are included in the flux observed along the line of sight of the CX-NPA even at a fixed toroidal and poloidal angle. The ratio of the loss trajectory is estimated by the collisionless-orbit calculation. Although the loss region along the CX-NPA's chord is largest in the case of B_{04}/B_{00} = 0.15 among the three configurations [9], the tail temperature and high-energy flux is largest in this case. This result suggests that the configuration with highest bumpy component is most favorable for the confinement of high-energy ions under this experimental condition. The same result has been obtained from the experiment that the charge exchange flux decay is measured to estimate the fast-ion confinement after the turning-off of the neutral beam [4]. This tendency is consistent with the fact that the neoclassical-diffusion coefficient in the collisionless region is smaller in the high bumpy configuration using the DKES code [3]. It is also expected from the discussion of the field structure that the grad-B drift is smallest in the configuration with the highest bumpy component [4].

The amplitude modulation [10] of the ICRF power is also performed for estimating the confinement of the fast ions. The injected ICRF power is modulated sinusoidally with a frequency of 100 Hz; then, the resultant change in hydrogen fluxes is observed. The phase difference between the injected ICRF wave and the charge exchange fluxes is determined from the measurement of CX-NPA. The phase delay is caused from the acceleration of fast ions by the ICRF wave, the friction between fast ions and bulk particles and the orbit loss of fast ions. The longer delay time corresponds to good confinement of fast ions since accelerated ions are lost slowly after the injection power decreases. 'Delay time' is defined as this phase delay, here. The delay time is considered to be an index of the fast ion confinement. Figure 4 shows delay time for the high bumpy case and the medium one. The delay time is longer in the high bumpy case in the energy range from 1 to 4 keV. For the low bumpy case, the delay time cannot be estimated since the flux is too small to estimate its phase. Lines in Fig. 4 are the calculated delay time from the Fokker-Planck equation [11] with additional loss terms corresponding to the transport and the orbit loss with a time constant τ_{Loss}. It is considered from this experiment that the confinement of the fast ions for the high bumpy ripple is longer than that for the medium bumpy ripple.

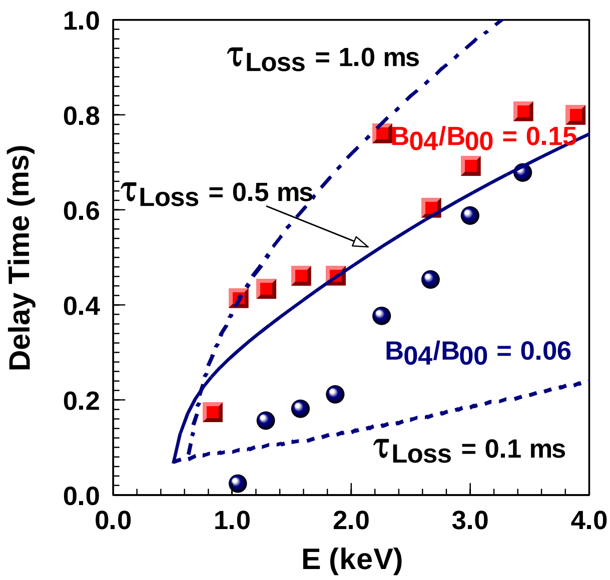

Fig. 4. The phase delay time between the injection wave and charge exchange fluxes for high and medium bumpy cases.

4. Dependence of the Bulk-Ion Temperature on the Bumpy Field Component

The bulk-deuteron temperature is evaluated from the deuterium flux observed by the CX-NPA. The two antenna loops are used for heating and the phase between the two-antenna currents is controlled in order to maximize the observed CX fluxes. The RF frequency is 23.2 MHz in the cases of B_{04}/B_{00} = 0.15 and 19 MHz for 0.06 and 0.01 as in the previous section. The line-averaged density before the ICRF pulse is about 0.4 x 10^{19} m^{-3} in all cases. The ion temperature before turning on the ICRF-pulse is in the range from 0.15 to 0.2 keV in an ECH plasma as shown in Fig. 5. The ion temperature is evaluated every 5 ms, and the bumpy component is 0.15 in this case.

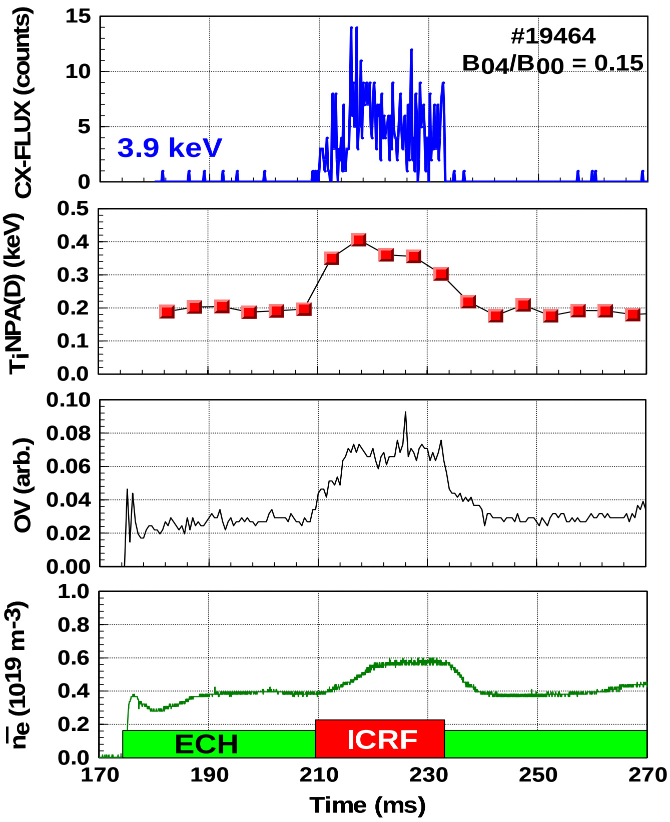

Fig.5. Time traces of the charge exchange flux (Hydrogen), T_i,,the oxytgen OV line emission and the density.

The ion temperature increases from 0.2 to 0.4 keV just after the ICRF pulse injection. The density is also raised during the ICRF pulse in this case. However, the density increase is negligible in most discharges. The line-emission from light impurities such as carbon or oxygen and metal impurities such as iron or titanium increases during the ICRF pulse.

The ion temperature increases with P_{ICRF} in the power range from 0.07 to 0.34 MW for three cases as shown in Fig. 6. Here, P_{ICRF} is the injected ICRF power at the position of the vacuum feedthrough. The increment of the ion temperature reaches 0.2 keV at the power of 0.3 MW in the high bumpy case. In the other cases, the temperature increase is lower than that in the high

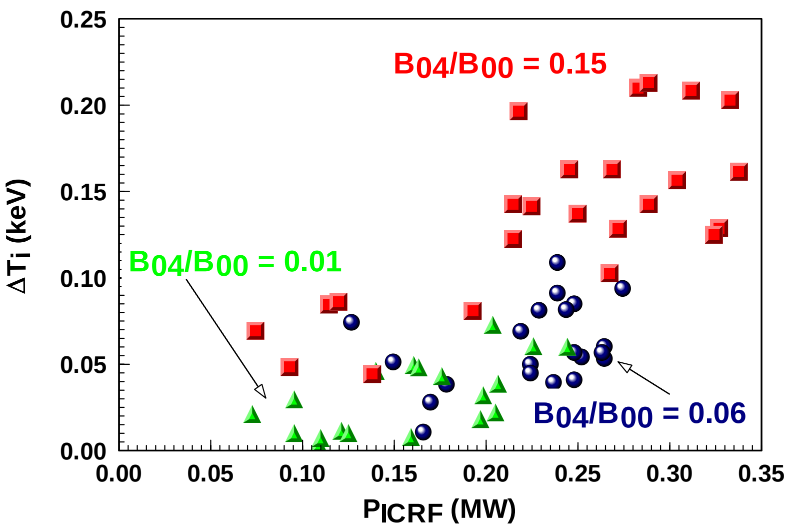

Fig. 6. Increase of the bulk ion temperature as a function of the injected ICRF power for three bumpy cases.

bumpy case. In the low bumpy case, it is less than 0.1 keV over this power range. The bulk-ion heating efficiency is also higher in the high bumpy case as well as the high-energy ion confinement. The bulk-ion heating in this heating scheme is performed through the Coulomb collisions with the high-energy minority ions produced by the ICRF heating. Therefore, the heating efficiency depends on the confinement of the high-energy ions as well as the bulk ions. It is considered that the energy transfer from the minority ions is larger in the high bumpy case since the high-energy tail is larger as mentioned in the previous section. In target ECH plasmas, the global energy confinement time is almost same for three configurations except the improved confinement mode [12]. Quantitative estimation of the energy transfer from the high-energy tail to bulk particles and the bulk-ion confinement for the various the bumpy components must be performed to understand this change of the heating efficiency.

5. Summary

A fast-ion formation and confinement experiment is performed using the ICRF minority heating in Heliotron J with the special emphasis on the effect of the bumpy component among the Fourier components of the magnetic field. Generated fast protons and bulk deuterons are detected by the CX-NPA whose energy range is 0.4 to 80 keV for protons and 0.2 to 40 keV for deuterons. High-energy ions are produced up to 10 keV by using two loop antennas installed on the corner section for ECH target plasma of a bulk-ion temperature of 0.2 keV and a line-averaged density of 0.4 x 10^{19} m^{-3}.

To clarify the role of the bumpy component in Heliotron J for the confinement of the high-energy ions, three configurations are selected: B_{04}/B_{00} = 0.01, 0.06 and 0.15. The observed tail temperature is highest in the high bumpy case under the conditions that the location of the cyclotron-resonance layer is adjusted within $\rho < 0.2$ and that the injection power and the density are kept constant. In the experiment of the amplitude modulation of ICRF power, the delay time as an index of the fast-ion confinement is also longer in the high bumpy case. It is considered that the bumpy control is effective for the fast-ion confinement in Heliotron J as expected in the theoretical prediction.

The increase of the bulk-ion temperature is observed in the ICRF experiment of Heliotron J. The ion temperature increases from 0.2 keV in the ECH plasma to 0.4 keV during the ICRF pulse. The increment of the ion temperature against the ICRF injection power is largest in the high bumpy case. The bulk-ion heating efficiency is also higher in the high bumpy case as well as the high-energy ion confinement. It is considered that the larger energy transfer from the higher tail temperature in the high bumpy case causes this better heating efficiency.

Acknowledgements

This work is performed with the support and under the auspices of the Collaboration

Program of the Laboratory for Complex Energy Processes, Institute of Advanced Energy, Kyoto University, the Kyoto University 21st century COE Program and the National Institute for Fusion Science (NIFS) Collaborative Research Program of NIFS04KUHL002.

References

[1] SANO, F., et al., “Experimental Program of Heliotron J”, J. Plasma and Fusion Res. SERIES **3** (2000) 26.

[2] OBIKI, T., et al., “First Plasmas in Heliotron J”, Nucl. Fusion **41** (2001) 833.

[3] WAKATANI, M., et al., “Study of a Helical Axis Heliotron”, Nucl. Fusion **40** (2000) 569.

[4] KOBAYASHI, S., et al., “Studies of High Energy Ions in Heliotron J”, Fusion Energy 2004 (Proc. 20th Int. Conf. Vilamoura, 2004), IAEA-CN-116/EX/P4-41, IAEA, Vienna (2005).

[5] HEINDBRINK, W.W., et al, “The Behavior of Fast Ions in Tokamak Experiments”, Nucl. Fusion, **34** (1994) 535.

[6] KWON, M., et al., “Fast Wave Heating Experiments in the Ion Cyclotron Range of Frequencies on ATF”, Nucl. Fusion **32** (1992) 1225.

[7] OKADA, H., et al., “Study of High Energy Particles Produced by ICRF Heating in Heliotron-E”, Nucl. Fusion **36** (1996) 465.

[8] MUTOH, T., et al., “Ion Heating and High-Energy-particle Production by Ion-cyclotron Heating in the Large Helical Device”, Phys. Rev. Lett. **85** (2000) 4530.

[12] OKADA, H., et al., “Formation and Confinement of High-Energy Ions in Heliotron J”, Fusion Sci. Technol. **50** (2006) 287.

[10] SAITO, K., et al., “A Study of High-Energy Ions Produced by ICRF Heating in LHD”, Plasma Phys., Control., Fusion **44** (2002) 103.

[11] STIX, T.H., “Fast-Wave Heating of a Two-Component Plasma”, Nucl. Fusion **15** (1975) 737.

[12] MIZUUCHI, T., et al., “Configuration Control for the Confinement Improvement in Helitoron J”, Fusion Sci. Technol. **50** (2006) 352.